Research Square

Preprints are preliminary reports that have not undergone peer review.
They should not be considered conclusive, used to inform clinical practice,
or referenced by the media as validated information.

Enhancing the Efficiency of Flexible Triboelectric Nanogenerators via Material Ratios and Surface Optimization for Wearable Electronics

Muskan Zaheer Mughal
International Islamic University, Islamabad
Gul Hassan
gulhassan.rahi5@gmail.com

International Islamic University, Islamabad
Arfa Asif
International Islamic University, Islamabad
Maryam Bibi
International Islamic University, Islamabad

Research Article

Keywords: Triboelectric nanogenerator, $BaTiO_3$, PDMS, energy harvesting, surface charge density, flexible electronics

Posted Date: April 20th, 2026

DOI: https://doi.org/10.21203/rs.3.rs-9279968/v1

License: This work is licensed under a Creative Commons Attribution 4.0 International License.
Read Full License

Additional Declarations: No competing interests reported.

Abstract

Triboelectric Nanogenerators (TENG) are devices that are gaining a lot of attention due to their ability to power low energy electronic devices. This study focuses on developing a flexible and efficient triboelectric nanogenerator that is capable of harvesting mechanical energy from various sources. The work also emphasize optimization of the device's efficiency by different fabrication and design approaches. Polydimethylsiloxane (PDMS), Barium titanate (BaTiO) and Nylon were the main materials used in the fabrication of the device. PDMS plays a role as a flexible material which is desirable for flexible devices while BaTiO is a ceramic with high dielectric constant which increases surface charge density of the TENG device. Nylon paired with PDMS maximizes the potential difference resulting in greater voltages. PDMS was prepared by 10:1 base-to-curing ratio of Sylgard 184 kit while sol-gel technique was used for the synthesis of the composite PDMS-BaTiO and dip coating was employed to deposit material on the electrodes. Nylon handkerchief was used as the material for second electrode as it serves as the electropositive layer in triboelectric layer. The fabricated set of devices achieved a maximum open circuit voltage of 1600V while the maximum current achieved was 180μA. The main findings of this research were that the device exhibited higher efficiency as compared to the previously reported work. An LED was successfully illuminated by the prepared device confirming its high charge generation capability. Thus, a high performance TENG device was successfully developed.

1. Introduction

Wearable technology (WT) has become a powerful instrument for gathering inexpensive, clinically useful data to improve patient evaluation [1]. This has raised the need for creative and effective energy sources to keep them operating. Wearable electronics are used in a variety of fields, including consumer electronics, textile technologies, and health technologies. All of these fields improve user experience and offer smooth integration into daily life [2]. Despite being widely employed as power sources, the limited lifespan, safety hazards (such as overheating), self-discharging, and high maintenance costs of traditional batteries in wearable electronics lower the devices' dependability and efficiency [3]. Renewable energy resources are an amazing approach for supplying power for wearable electronic devices that has the potential to replace the frequent dependency on batteries. Triboelectric nanogenerators initially introduced by Wang et al. (2012) is an emerging technology for this energy harvesting mechanism.[4], used to covert mechanical energy into electricity. By harnessing the triboelectric effect and electrostatic induction, they enable continuous, self-sufficient energy harvesting, minimizing the need for frequent battery replacements [5]. TENG are usually made of polymers (PDMS, PTFE, and PVDF), providing flexibility and enabling efficient energy harvesting. For hybrid approaches ceramic fillers are often incorporated to enhance dielectric properties. TENG can be designed to be stretchable, biodegradable, bioabsorbable, or implantable, catering to the diverse needs of modern wearable technology [6]. In this study PDMS was used for flexibility, $BatiO_3$ for dielectric properties and Nylon for enhancing potential efficiency for improving the device. **Hassan et.al** [7] fabricated a piezoelectric nanogenerator that has the capability of generating significant electrical output for

mechanical stimuli. **Mao et.al** [8] (2025) fabricated TENG that achieved 6.52-fold power density increase that is the power density of 4.37 W/m^2. **Xie et.al** [9] (2025) focus on the review on development of graphene based electrodes in TENG. The results obtained from this review was that electron skin can be produced with high pressure sensitivity of 78.4k/Pa. the response time of 1.4 ms. **Li et.al** [10] (2025) worked on fabrication a triboelectric nanogenerator that gave high short circuit current, open circuit voltage and output power and are capable of self-healing. **Zhao et.al** [11] (2025) focused on the development of high-performance TENG that improved performance with 61.48% open circuit voltage, 77.11% short circuit current and 46.16% short circuit charge while thermal stability was maintained at 60ºC. **Yang et.al** [12] (2025) fabricated a device with electrical conductivity observed to be 5.27 S/m while the sensitivity was 0.268k/Pa. The electrical output obtained from the device was open-circuit voltage of 223.32V and power density of 4.20 W/m^2. **Deng et.al** [13] (2025) fabricated a device with maximum current output to be 0.215 μA and voltage of 210V under condition of 3 Hz, 9N force and 8mm displacement. **Lee et.al** [14] (2025) Fabricated a device which had an output voltage of about 421.06 V which is 1.96% improved while the output current is 32.33 μA that is 2.67% improved. **Yue et.al** [15] (2024) fabricated a device with an open circuit voltage of 85V and power density of 4.2 W/m^2. **Ali et.al** [16] fabricated a hybrid self-healing nanogenerator that demonstrated significant electrical properties, harvested energy from wind and was able to power multiple LED. **Hassan et.al** [17] fabricated a hybrid nanogenerators achieving high voltage, power density and current density making it suitable for wireless sensor network. Despite their potential, triboelectric nanogenerators (TENGs) have issues with stability and efficiency in real-world settings. One of those are that their long-term use require improved quality as overtime use reduces performance. They usually produce high voltage but attaining high current is a difficult task and a sable energy is required. Improving these factors can enhance the overall efficiency of the device.[13]. Many studies have reported that achieving high flexibility in TENG is still a challenge and the study aims on achieving flexibility and efficiency. This can be done by exploring different structural designs and combined materials and designs. The main focus is to improve both performance and wearability.

This study proposes the fabrication and optimization of a flexible triboelectric nanogenerator. The device is fabricated by using PDMS as the primary triboelectric layer as it shows excellent triboelectric properties. $BaTiO_3$ nanoparticles were incorporated into PDMS in order to improve its dielectric properties. As a result, the composite not only improve electrical properties of the device but also enhance the performance and efficiency of the device. The device fabricated using these materials produces a maximum voltage of 1550 V and current of about 180 μA. The final device showed an efficiency of 64.3% which can be an exceptional source for energy harvesting applications.

2. Experimental section

2.1 Materials

Barium Titanate ($BaTiO_3$) nanoparticles 99% pure purchased from maklin china and used without further purification. Sylgard 184 kit was purchased from United States and was used for the fabrication of PDMS. Nylon handkerchief was used to act as triboelectric positive layer in a device.

2.2 Material Synthesis and fabrication process

For the synthesis of device first of all we prepared PDMS solution by adding 10:1 ratio of base and curing agent in a beaker. The solution is then mixed thoroughly by using a magnetic stirrer. Four different devices were prepared by employing different methodology. The synthesis process of TENG device is mentioned below in Fig. 1. Detailed schematics of synthesis is provided in supplementary data S1, S2 and S3.

After the preparation of PDMS solution, PDMS layers with varying thicknesses were then cast onto aluminum foil. The sample was then cured at 100ºC to obtain a non-sticky solid PDMS film. Once cured, the device was assembled. 3 devices with different thicknesses were fabricated by using same method. The devices were tested to evaluate their electrical performance. The second set of devices was prepared by varying the $BaTiO_3$ content in PDMS matrix. Five different ratios were tested in this process. Initially 1g $BaTiO_3$ was added to the solution of PDMS to observe the changes in current and voltage as compared to the previous devices. The solution containing PDMS and $BaTiO_3$ was then cured on aluminum foil and assembled to evaluate the required electrical output. After that the ratio was increased to 2g, 3g, 4g and 5g respectively using the same procedure. The third set of devices was fabricated using the optimal PDMS-BTO composite ratio, identified based on the best-performing results. This composite was applied to one electrode, while the other electrode utilized activated nylon. The nylon cloth was activated by soaking it in a dilute NaOH solution for 30 minutes. After that activated nylon was rinsed multiple time and then dries in order to remove residual NaOH. The second electrode was previously fabricated PDMS-BTO. The device was then assembled to check electrical properties. The fourth set of devices was fabricated by using the optimized layer of PDMS-BTO and then allowing mold on the uncured layer to create patterns. Once the material was cured completely, the mold was removed. The device was then assembled and tested for electrical properties.

2.2 Characterization

The morphologies of the samples were characterized by scanning electron microscopy (KYKY-EM/6900 SEM) and X-ray Diffraction instrument (DW-XRD-Y3000). The electrical characteristics of triboelectric nanogenerator were analyzed using Keysight B2983A and Hantek DSO2C10.

3. Results and Discussion

XRD analysis of pure PDMS, pure Barium titanate and composite PDMS-BTO was performed. Pure barium titanate showed a crystalline tetragonal structure with a sharp peak at (100). Peaks remained stable at different weight fraction. Pure PDMS showed board hump and wide peaks due to its amorphous behavior. And due to their polymeric nature they do not have any JCPDs cards. The final XRD

pattern is of composite PDMS-BTO. The pattern shows both sharp peaks and a broad hump, confirming the successful blending of nanoparticles into the polymer. The sharp peaks indicate an increase in crystallinity due to the addition of $BaTiO_3$. The unchanged position of the broad hump suggests that there is no major change in the structure of the PDMS matrix.

Nanocluster like structures were observed in SEM image of pure BTO sample. The diameter is observed to be near 253nm while particle size range from 225 to 384nm. The surface morphology of pure PDMS was observed in this sample using Scanning electron microscopy. Highly uniform and smooth surface was observed with no observable phase segregation or defects. The visual smoothness implies successful curing and minimal external contamination and mechanical handling and contributes in sustainability and soft electronic applications where homogeneity is critical. The surface morphology of composite of $BaTiO_3$ confirms a general uniform dispersion of $BaTiO_3$ nanoparticles throughout PDMS matrix. The effective mixing of $BaTiO_3$ shows that they are compatible and are mixed properly. This uniform dispersion enhance the performance, which is likely to lead consistent dielectric and mechanical properties

Energy-Dispersive X-ray Spectroscopy (EDX) was employed to analyze the elemental composition of the PDMS matrix embedded with barium titanate ($BaTiO_3$) particles. Successful incorporation of $BaTiO_3$ nanoparticles within the polymer network of PDMS was confirmed. The EDX spectra reveal the presence of Silicon, oxygen, carbon, barium, and titanium confirming the presence of $BaTiO_3$. A peak of iron (Fe) was detected in some areas that is likely due to contamination during sample preparation as shown below in Fig. 5.

To enhance the performance of the triboelectric nanogenerator (TENG), the PDMS layer thickness was varied between 0.415 mm and 0.115 mm. It was observed that reducing the thickness resulted in a clear increase in output voltage. The highest voltage in this case was obtained at 500 V and was recorded at 0.115 mm, while the lowest, 90 V, was observed at 0.415 mm. The output current was also measured for different PDMS thicknesses to observe the effect on the electrical performance of the TENG. It was found that the current increased noticeably as the thickness decreased. The highest current obtained in this set of devices was 50 μA that was obtained at thickness of 0.115mm. The lowest current was obtained at 0.415mm that was 8 μA. It was observed thinner layer improve not only current but also voltages enhancing the output efficiency. Higher charge density contribute to higher current that was also observed by Gomes et al.[21] The maximum voltage in this trend was observed is 500V and highest current was at 50 μA. voltages and currents were observed under different conditions which was then used to estimate a maximum power of 6.24 mW.

For further optimization BTO was added in order to enhance the efficiency of the device. The concentration of nanoparticles ranged from 1g to 5g. On increasing the concentration of BTO voltage along with current increased until 3g but drop after that. This happened because when added too many nanoparticles, they do not mix properly and start forming clogs which reduce the performance of the device. The highest voltage of 560 V and 180 μA was recorded when the ratio of BTO was 3g, while the

lowest, 250 V and 59 μA, was observed at concentration 5g. the maximum voltage obtained in this trend was 560V and highest current was 180 μA. Similar as the previous trend current and voltages ware recorded under different conditions which were then used to calculate maximum power of 25.2 mW. Mechanical input was determined as the tapping force in this case was 10N foam separator was of 2mm. the estimated input power was 25.25mW giving efficiency of about 50.2%.

In this set of devices nylon was selected as an electropositive layer for optimization, PDMS-BTO was electronegative layer in this case. For this nylon was treated with dilute NaOH for 30 minutes for activation. After activation of nylo, it was dried and assembled in device. This configuration resulted in a significant increase in output voltage, with a peak voltage of 950 V observed. However, the current dropped to 12 μA, likely due to internal resistance or less efficient charge transfer at the interface. The power calculated from these values was approximately 2.85 mW, while the efficiency based on an estimated mechanical input of 40 mW was calculated to be around 5.7%. Although the voltage output improved, the overall efficiency decreased due to the substantial reduction in current.

For further optimization, differen.t molds were used on the layer of PDMS-BTO composite for modifying surface roughness. Four types of molds were used for this purpose which gave different patterns on the surface after curing. A plastic mold, a red camlet cloth, a disposable cloth bag and a cloth bandage. The lowest output obtained among these molds was the bandage one as it gave 1100 V voltage and 3.4 μA. The cloth bag mold gave voltage of 1500V but the current was only 6.5 μA. The red camlet cloth gave the highest voltage of about 1600V but the current was low due to surface contact quality. The highest output obtained was from plastic mold, it not only gave good voltage but also good current. The voltage obtained was 1550V and the current was 83 μA which was the best one out of all. So the power and efficiency of the best device was calculated. The power generated by this device was 32.16mW. For the calculation of efficiency the mechanical input power was estimated to be 40mW, giving device and efficiency of about 64.3%. Mold texture clearly affected both voltage and current, which impacted overall performance.

For verification that the optimized TENG can power a real-life electronic component, a circuit consisting of a full-wave bridge rectifier, a capacitor, a resistor, and a red LED was used as shown in schematic Fig. 9. The AC output from the TENG was connected directly to the rectifier, which converted it into DC. This DC voltage was stored in the capacitor, with the LED connected across it. Upon repeated tapping of the device, the capacitor gradually charged as shown in Video 1. Once sufficient voltage was accumulated, the red LED illuminated, confirming that the device produced usable electrical energy. This showcase the results that a TENG can operate low power devices and can be used in harvesting applications.

4. Conclusion

In this study, a PDMS-BTO based TENG device was developed and optimized. This study influence the thickness of PDMS, different BTO concentration and surface treatment by using different kind of molds.

The optimized device showed a peak voltage of 1550 V while the optimized short circuit current was 83 μA. the estimated power output calculated for the optimized case was 32.16mW that provided the efficiency of 64.3%. A rectifier-capacitor circuit was used in order to check whether the device is suitable for practical use or not. A red LED was glowed showing the device feasibility in real-time device. Future work on this study focuses on integrating TENG with storage devices. Moreover further design refinement is needed for real-world applications. Potential used of this device is wearable electronics, sensors and environmental energy harvesting.

Declarations

Funding and Acknowledgment

This work is supported by the National Research Program for Universities- NRPU (20-15054/NRPU/R&D/2021 2021) funded by higher Education of Pakistan.

Declaration of Competing Interest

All the authors contributed to this research work have no conflict of interest.

Research Data Policy and Data Availability Statement

Data will be made available on reasonable request.

Author Contribution

M.Z.M and G.H conceived the research. M.Z.M designed, fabricated the device, performed experiment and took the measurements. M.Z.M and A.A analyzed the measured data. M.Z.M, M.B, A.A and G.H prepared the manuscript and discussed the results.

References

1. A. Godfrey, V. Hetherington, H. Shum, P. Bonato, N.H. Lovell, S. Stuart, From A to Z: Wearable technology explained. Maturitas. **113**, 40–47 (Jul. 2018). 10.1016/j.maturitas.2018.04.012
2. M. Çİçek, WEARABLE TECHNOLOGIES AND ITS FUTURE APPLICATIONS, vol. 3, no. 4
3. A. Riaz, M.R. Sarker, M.H.M. Saad, R. Mohamed, Review on Comparison of Different Energy Storage Technologies Used in Micro-Energy Harvesting, WSNs, Low-Cost Microelectronic Devices: Challenges and Recommendations. Sensors. **21**(15), 5041 (Jul. 2021). 10.3390/s21155041
4. Z.L. Wang, Nanogenerators, self-powered systems, blue energy, piezotronics and piezo-phototronics – A recall on the original thoughts for coining these fields. Nano Energy. **54**, 477–483 (Dec. 2018). 10.1016/j.nanoen.2018.09.068

5. Y. Wang, Y. Yang, Z.L. Wang, Triboelectric nanogenerators as flexible power sources. Npj Flex. Electron. **1**(1) (Nov. 2017). 10.1038/s41528-017-0007-8
6. X. Pu, C. Zhang, Z.L. Wang, Triboelectric nanogenerators as wearable power sources and self-powered sensors. Natl. Sci. Rev. **10**(1), nwac170 (Jan. 2023). 10.1093/nsr/nwac170
7. S. Ejaz, G. Hassan, A. Shuja, Fabrication and Characterization of Piezoelectric Nanogenerator Based on ZnO and PVP for Harvesting Energy System Applications. J. Mater. Sci. Mater. Electron. **36**(12), 695 (Apr. 2025). 10.1007/s10854-025-14783-2
8. J. Mao, Y. Wen, X. Feng, W. Xu, S. Seo, Multi-Sized porous silica/PDMS composite layer for enhanced performance in triboelectric nanogenerators. Appl. Surf. Sci. 162291 (Jan. 2025). 10.1016/j.apsusc.2025.162291
9. B. Xie et al., Advances in Graphene-Based Electrode for Triboelectric Nanogenerator. Nano-Micro Lett. **17**(1) (Dec. 2025). 10.1007/s40820-024-01530-1
10. Z. Li et al., Metal coordination bond and rough interface enhanced triboelectric nanogenerator aiming for multiple complex conditions. Nano Energy. **134**, 110532 (Feb. 2025). 10.1016/j.nanoen.2024.110532
11. Y. Zhao et al., Extreme environment-resistant high performance triboelectric nanogenerator for energy harvesting and self-powered positioning system. Nano Today. **61**, 102616 (Apr. 2025). 10.1016/j.nantod.2024.102616
12. Q. Yang et al., Triboelectric nanogenerator based on well-dispersed and oxide-free liquid metal-doped conductive hydrogel as self-powered wearable sensor for respiratory and thyroid cartilage signal monitoring. Nano Energy. **134**, 110530 (Feb. 2025). 10.1016/j.nanoen.2024.110530
13. X. Deng et al., Preparation and properties of triboelectric nanogenerator based on PVDF-TrFE/PMMA electrospun film. Adv. Compos. Hybrid. Mater. **8**(1), 19 (Feb. 2025). 10.1007/s42114-024-01103-1
14. K. Lee, S. Park, K. Jung, I. Yong Moon, J.H. Ryu, K.M. Kim, Enhanced performance of polydimethylsiloxane-based triboelectric nanogenerator using BaTiO3/MWCNTs. J. Cryst. Growth. **649**, 127952 (Jan. 2025). 10.1016/j.jcrysgro.2024.127952
15. O. Yue et al., Auxetic Structure-Assisted Triboelectric Nanogenerators for Efficient Energy Collection and Wearable Sensing. Adv. Energy Mater. **14**, 2400212 (Jun. 2024). 10.1002/aenm.202400212
16. I. Ali, G. Hassan, A. Shuja, Fabrication of self-healing hybrid nanogenerators based on polyurethane and ZnO for harvesting wind energy, *J. Mater. Sci. Mater. Electron.*, vol. 33, no. 7, pp. 3982–3993, Mar. 2022, 10.1007/s10854-021-07591-x
17. G. Hassan, F. Khan, A. Hassan, S. Ali, J. Bae, C.H. Lee, A flat-panel-shaped hybrid piezo/triboelectric nanogenerator for ambient energy harvesting. Nanotechnology. **28**, 175402 (Apr. 2017). 10.1088/1361-6528/aa65c3
18. Z.L. Wang, Triboelectric nanogenerators as new energy technology and self-powered sensors – Principles, problems and perspectives. Faraday Discuss. **176**, 447–458 (2014). 10.1039/C4FD00159A

19. B. Mikolaszek, J. Kazlauske, A. Larsson, M. Sznitowska, Controlled Drug Release by the Pore Structure in Polydimethylsiloxane Transdermal Patches, *Polymers*, vol. 12, no. 7, p. 1520, Jul. 2020, 10.3390/polym12071520
20. S. Nayak, T.K. Chaki, D. Khastgir, Development of Flexible Piezoelectric Poly(dimethylsiloxane)–$BaTiO_3$ Nanocomposites for Electrical Energy Harvesting. Ind. Eng. Chem. Res. **53**(39), 14982–14992 (Oct. 2014). 10.1021/ie502565f
21. A. Gomes, C. Rodrigues, A.M. Pereira, J. Ventura, Influence of Thickness and Contact Area on the Performance of PDMS-Based Triboelectric Nanogenerators, Mar. 27, 2018, *arXiv*: arXiv:1803.10070. Accessed: Sep. 17, 2024. [Online]. Available: http://arxiv.org/abs/1803.10070

Figures

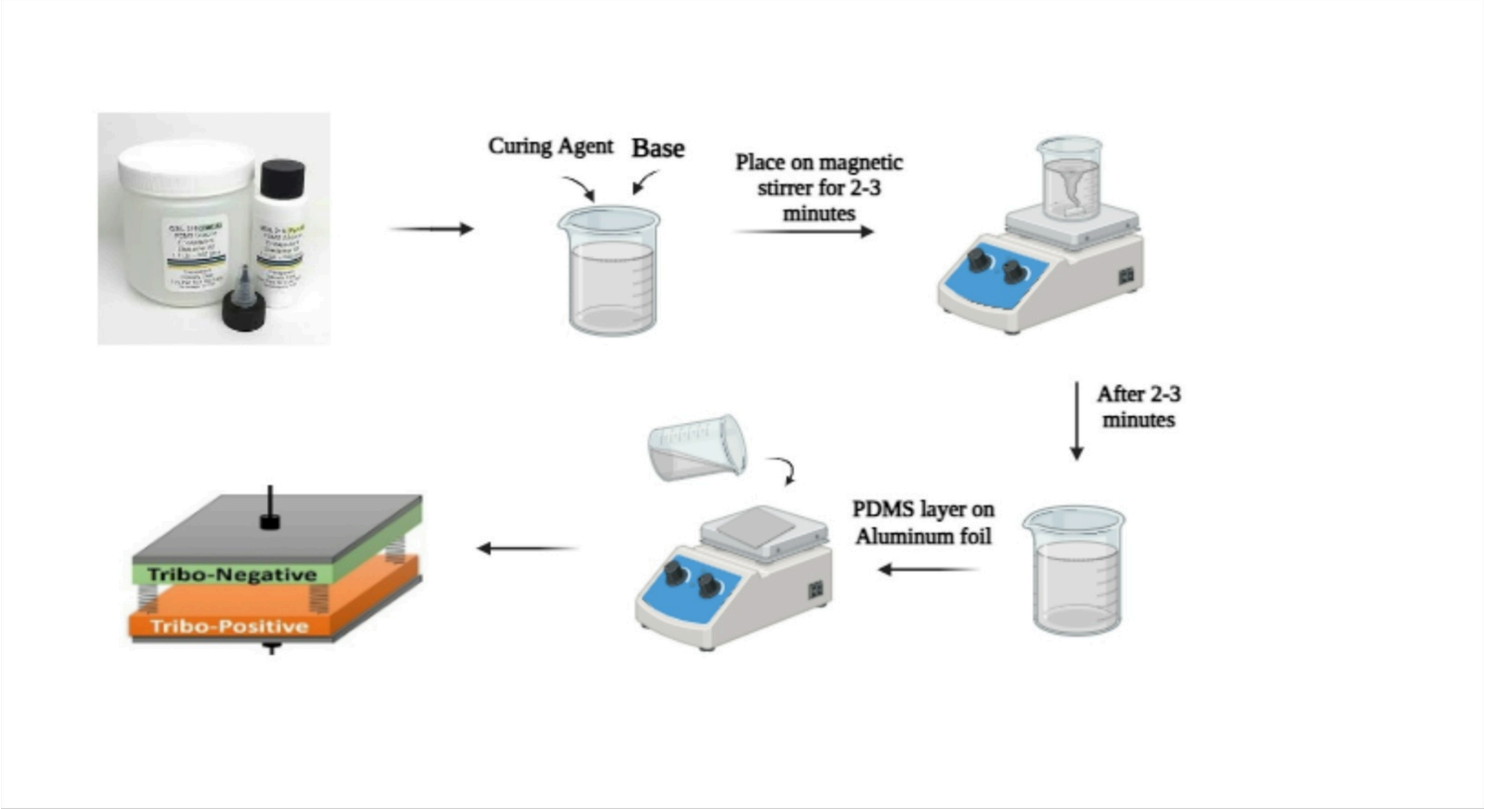


Figure 1

Synthesis process of Polydimethylsiloxane slurry

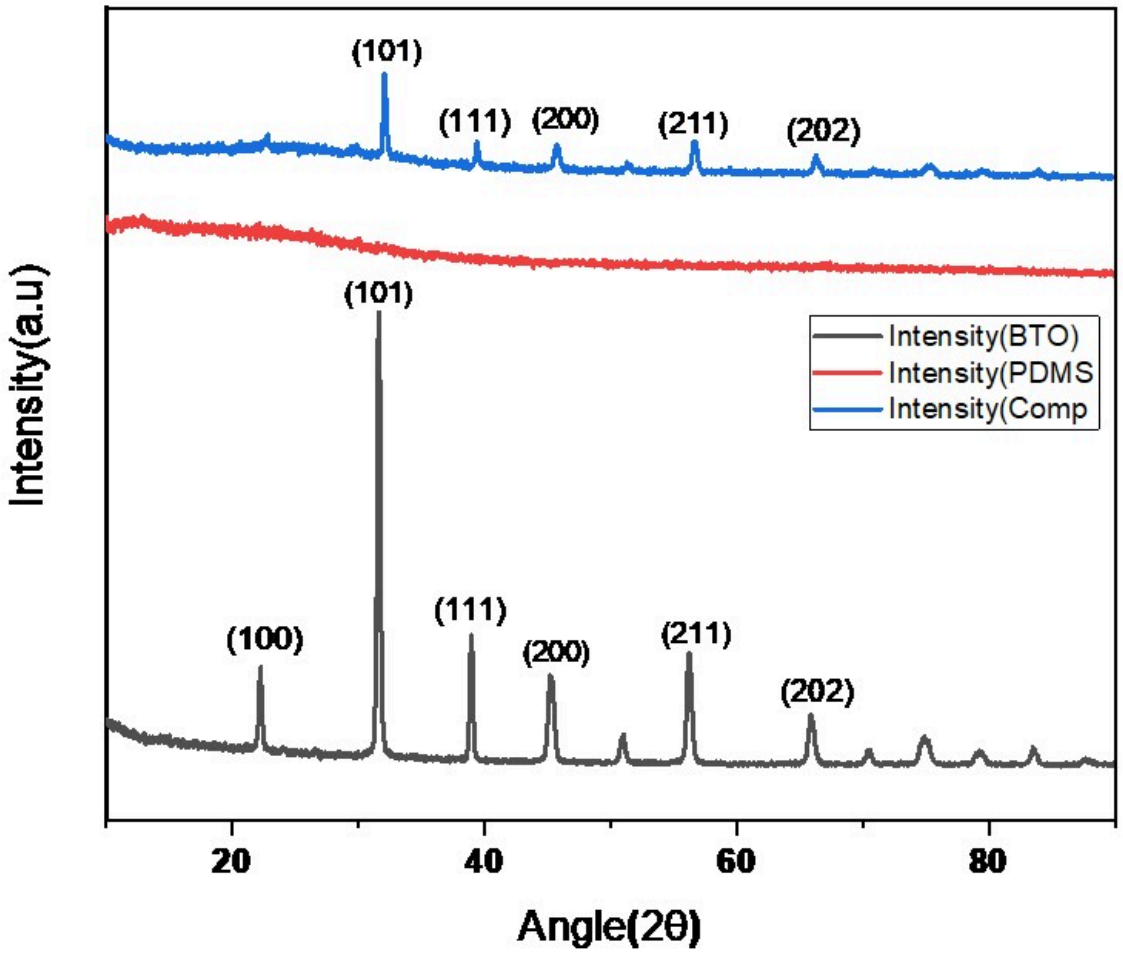


Figure 2

XRD Analysis of pure BTO, Pure PDMS and Composite BTO-PDMS

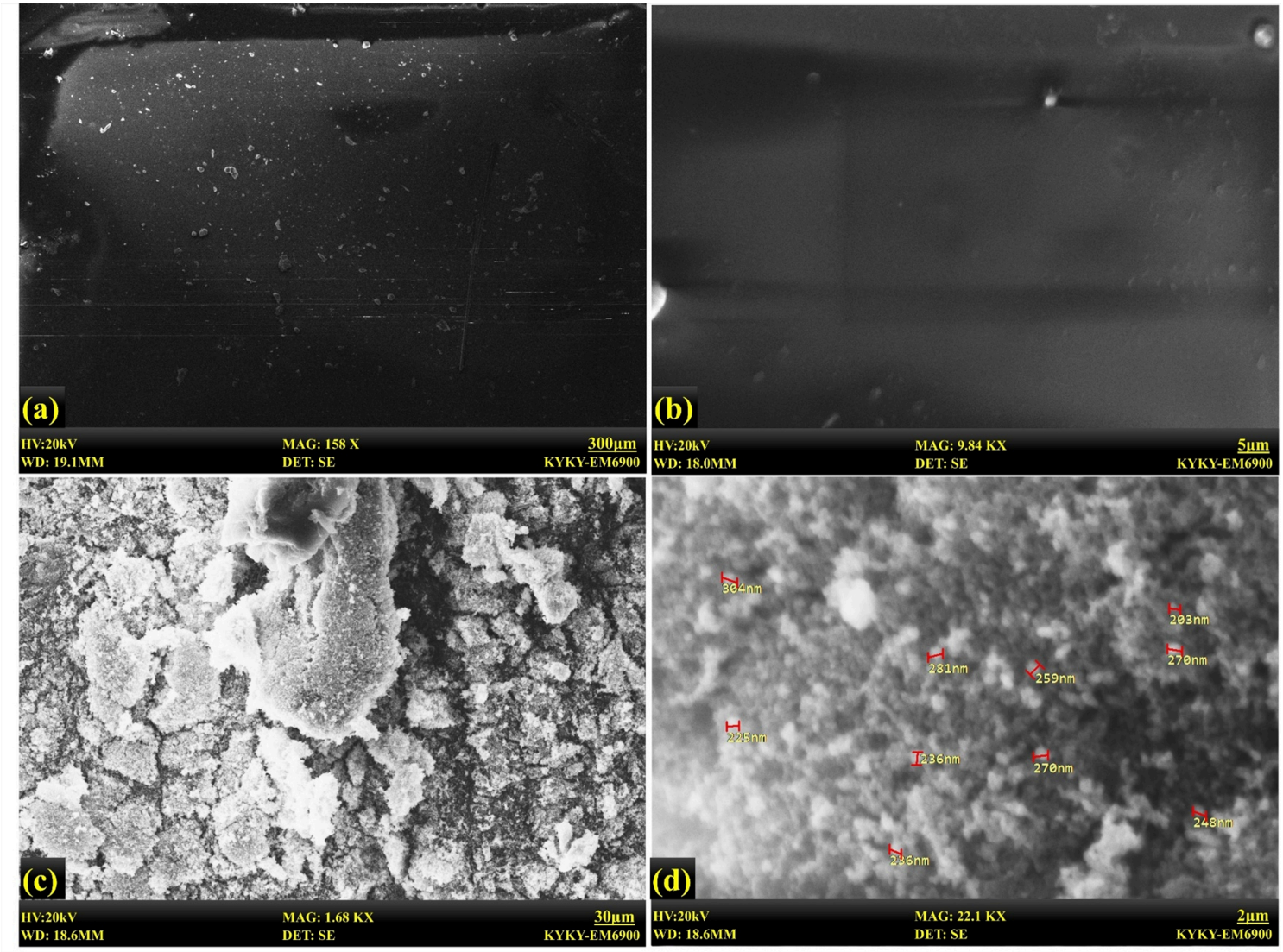
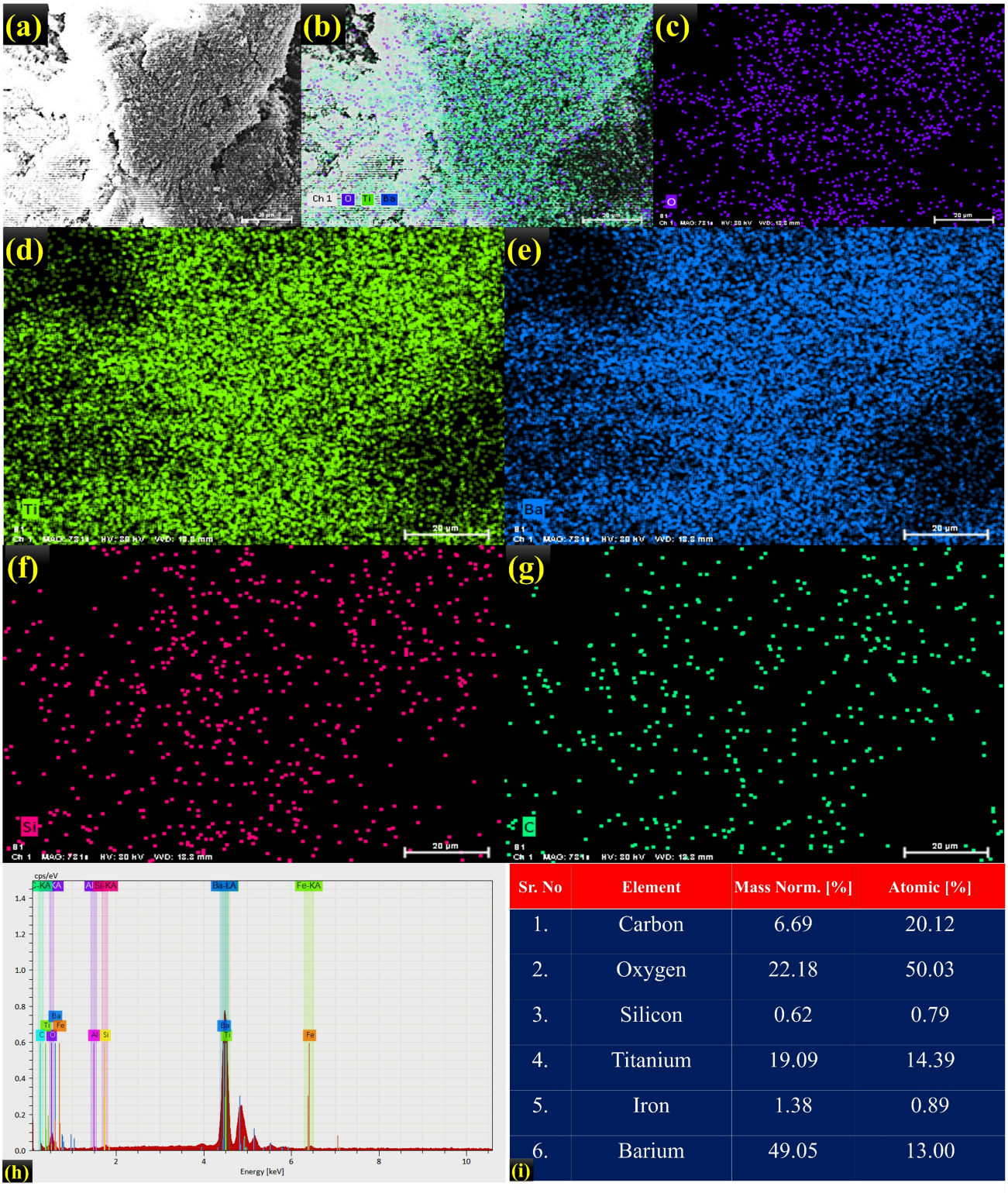


Figure 3

(a) SEM analysis of composite PDMS-BTO under 300um **(b)** Pure PDMS **(c)** Pure BTO observed under 30um **(d)** Observed average diameter (253nm) of BTO NPs under 2um



Sr. No	Element	Mass Norm. [%]	Atomic [%]
1.	Carbon	6.69	20.12
2.	Oxygen	22.18	50.03
3.	Silicon	0.62	0.79
4.	Titanium	19.09	14.39
5.	Iron	1.38	0.89
6.	Barium	49.05	13.00

Figure 4

(a) SEM image for EDX analysis **(b)** Elemental mapping of Ti, O and Ba **(c-g)** Distribution of elements via multiple colors **(h)** EDX spectra comprising of Ba and Ti peaks **(i)** Atomic & Mass Percent distribution of elements

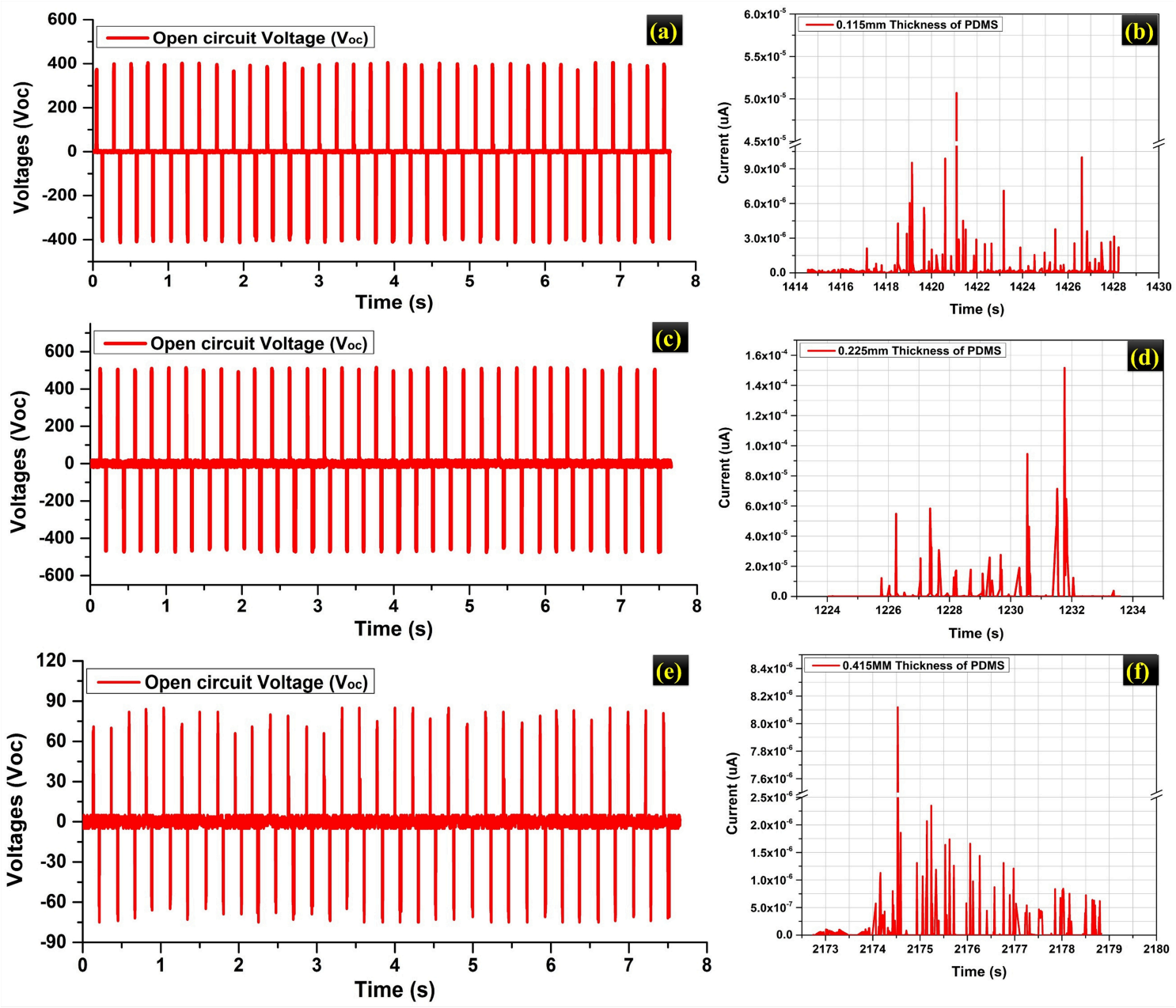


Figure 5

Voltage and currents at the thickness of **(a-b)** 0.115mm **(c-d)** 0.225mm **(e-f)** 0.415mm

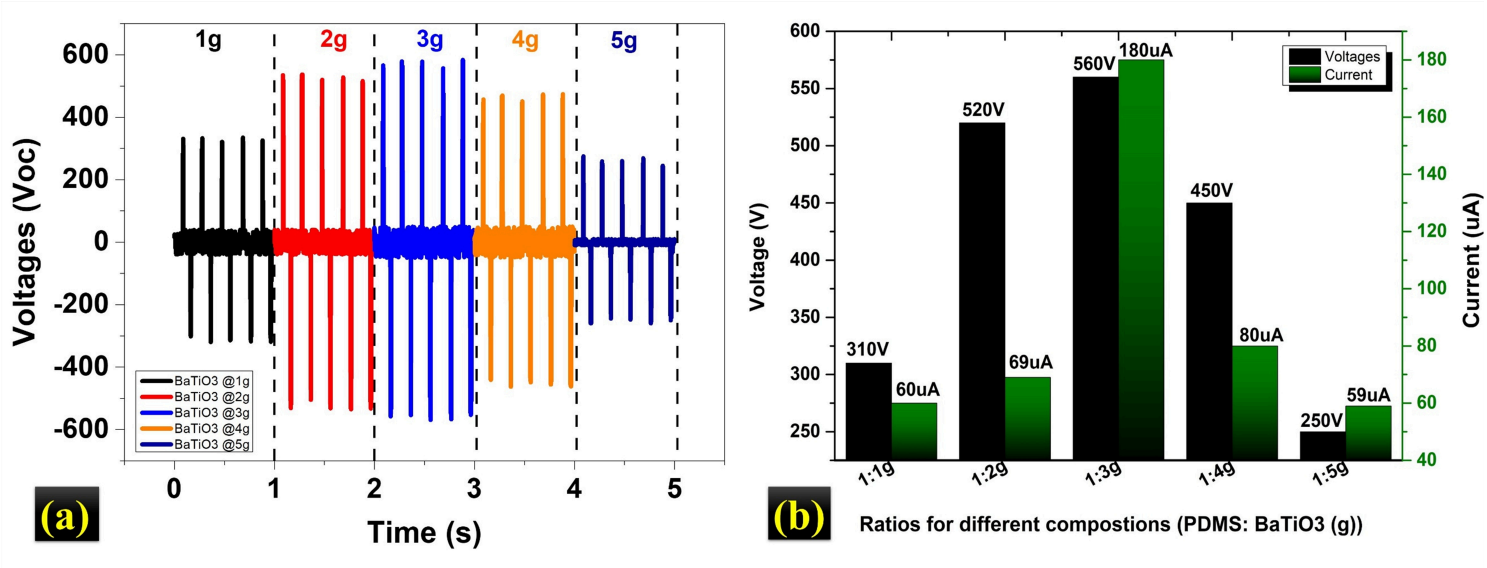


Figure 6

Variations on multiple ratios of PDMS/BatiO_3 **(a)** Voltages **(b)** Currents

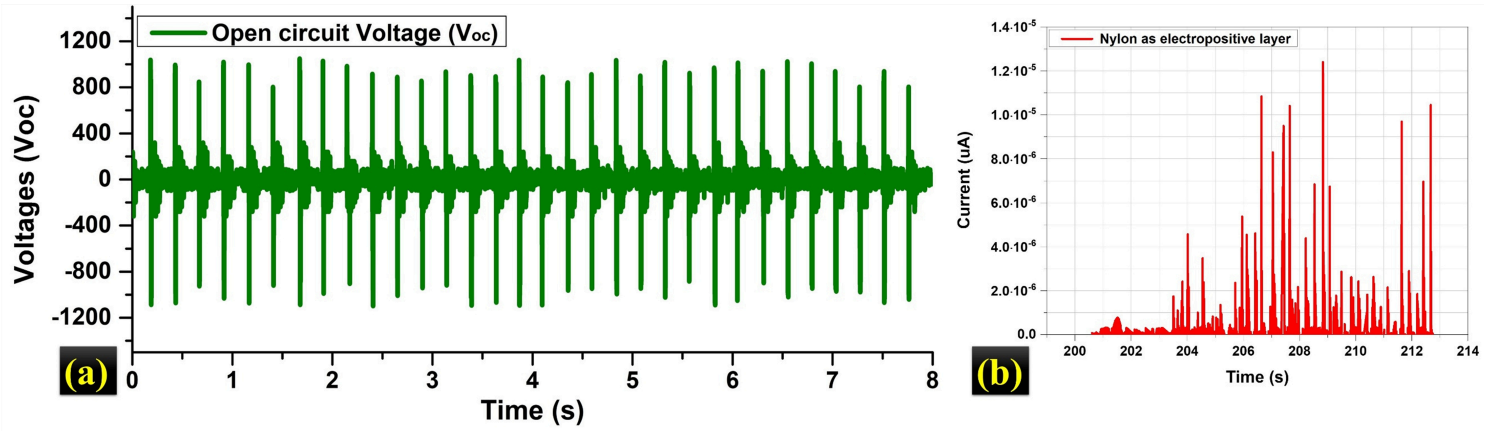


Figure 7

Nylon Mold as electropositive layer in TENG with **(a)** Voltage@950V **(b)** Current@12uA

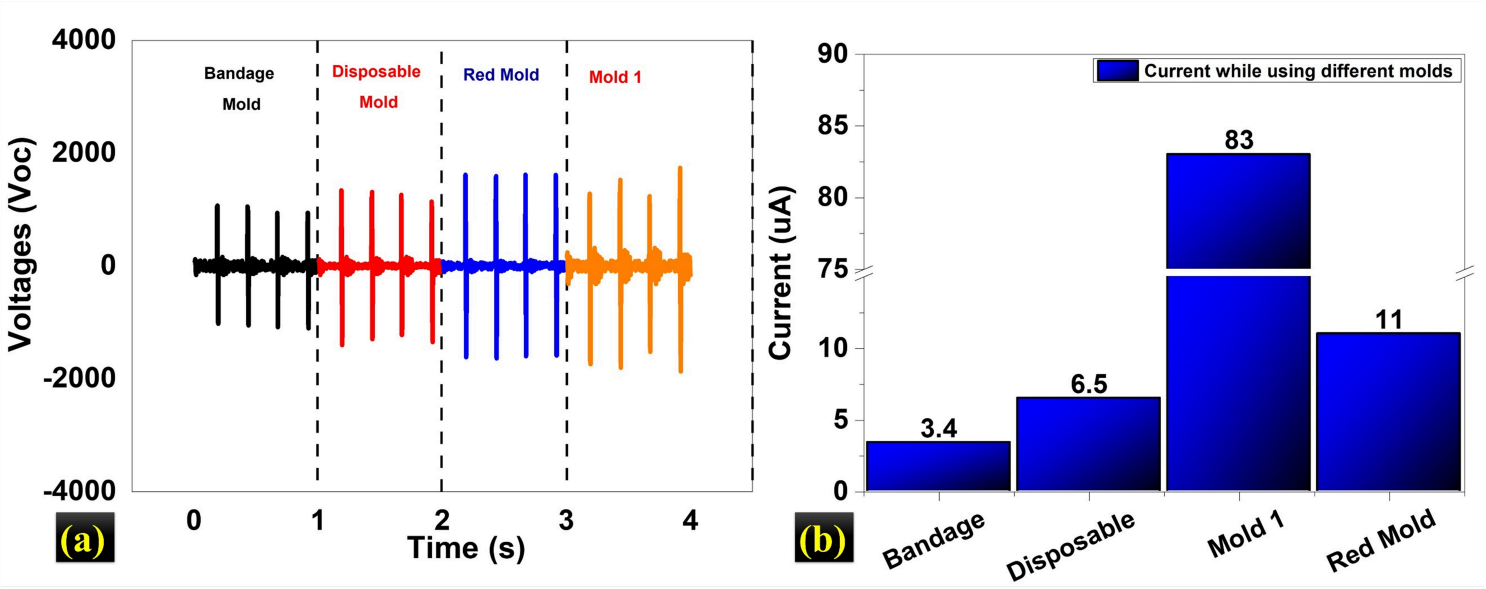


Figure 8

(a-b) Trend of Voltages and currents plotted comprising multiple molds

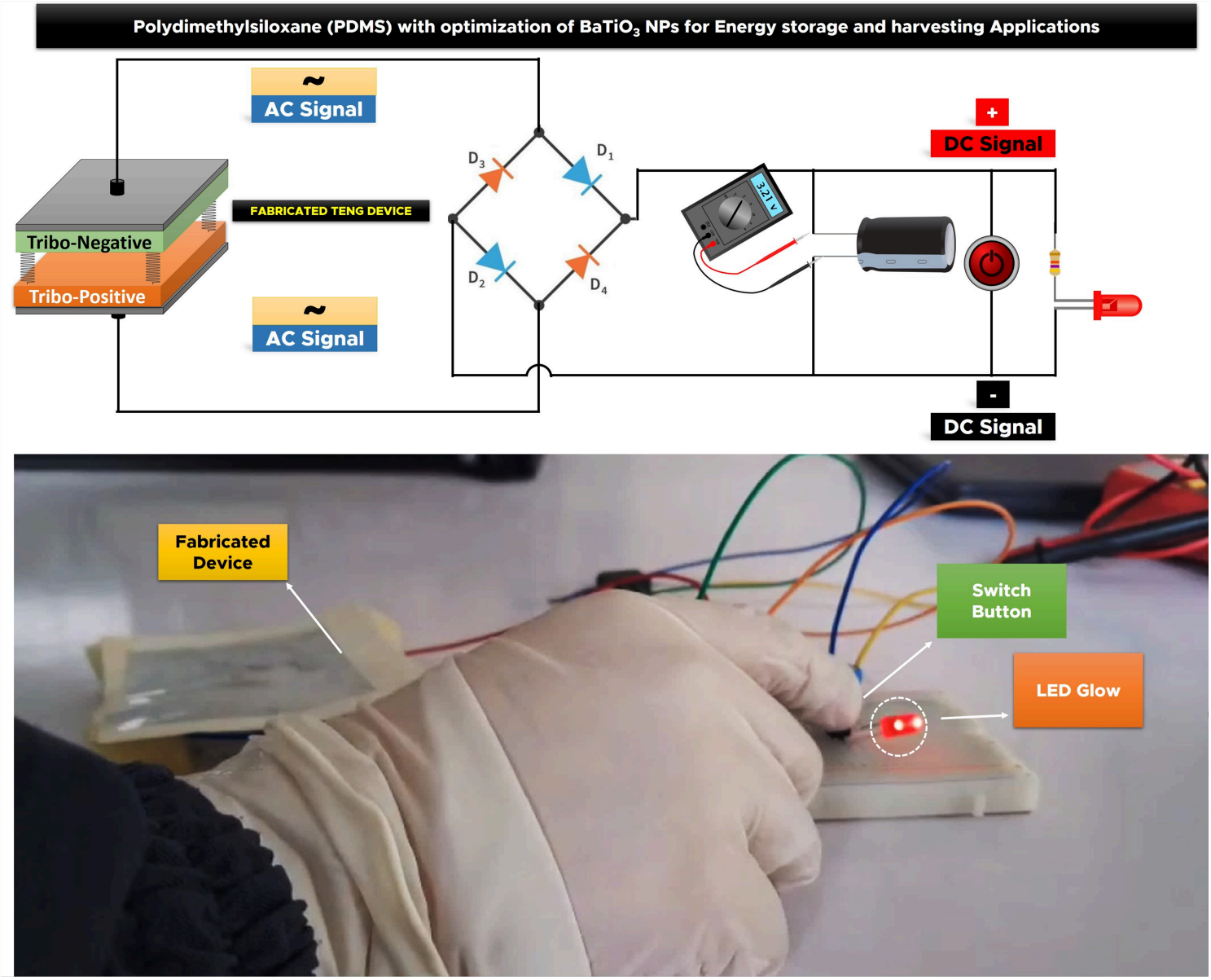


Figure 9

(a) Schematic representation of fabricated TENG and rectifier circuit **(b)** Experimental setup showing LED illumination by the fabricated device.

Supplementary Files

This is a list of supplementary files associated with this preprint. Click to download.

- SupplementaryData.docx
- Graphical.png